ORIGINAL RESEARCH

On the iso-conversional analysis of the activation energy of amorphous-crystalline transition in nano-crystalline Se-Te-In-Pb chalcogenide glasses

Article history:
Received: 21-08-2024
Revised: 19-09-2024
Accepted: 20-09-2024
Published: 10-11-2024

Aayush Kainthla[a], Shubham Sharma[a], Meenakshi[a], Sangam Kapoor[a], Anjali[b], Nagesh Thakur[a], Balbir Singh Patial[b,*]

Abstract: The present paper examines the fluctuations in activation energy of amorphous-crystalline phase transition of $Se_{79-x}Te_{15}In_6Pb_x$ (x = 0, 1, 2, 4, 6, 8 and 10) chalcogenide glasses using computational iso-conversional analysis for the data obtained under non-isothermal conditions using differential scanning calorimetric technique at four different heating rates; 5, 10, 15 and 20 K/min. This study examines how the activation energy of crystallization (E_c) varies with the degree of conversion (χ) and temperature (T) using an algorithm developed in Python named as *HPU-B-MASS*. The Python algorithm incorporates iso-conversional methods; Kissinger-Akahira-Sunose (KAS), Ozawa-Flynn-Wall (OFW), Tang & Chen and Starink methods to analyze the variation of E_c with both χ and T. It is found that E_c is not constant but varies with χ as well as T. The iso-conversional analysis of the investigated glasses indicates that the assumption of constant E_c is not appropriate. E_c obtained for the investigated alloys from different methods are different. This difference can be attributed to the fact that these methods are based on approximations involved in obtaining the final equation of different formalisms. Furthermore, our findings suggest an increased propensity for crystallization in glasses with Pb content as compared to the parent ternary alloy.

Keywords: Chalcogenide glasses; Differential scanning calorimetry; Non-isothermal methods; Iso-conversional analysis; Computational analysis.

INTRODUCTION

In recent years, chalcogenide glasses have become the focus of attention, primarily owing to their crucial characteristics, like broad transmission range, elevated refractive index ($2.0 \geq n' \geq 3.7$), excellent resistance to chemical wear, effective optical transition, high photosensitivity, a high second/third-order optical nonlinearity, transparency in both the mid and extended infrared ranges, coupled with reduced phonon energy in comparison to fluoride or oxide glasses and amorphous-crystalline (a-c) phase transition (Wuttig *et al.*, 2017; Kumar *et al.*, 2011; Lankhorst *et al.*, 2005; Zakery & Elliott, 2003; Vashist *et al.*, 2023; Liu *et al.*, 2001). Therefore, chalcogen-based glasses have drawn substantial interest in the fields of science and technology owing to their numerous potential applications. These include xerography, switching, chemical sensing, memory devices, near-field scanning microscopy/spectroscopy, photolithographic processes, infrared

[a] Department of Physics, Himachal Pradesh University Summerhill, Shimla, 171005, H.P., India.
[b] School of Basic and Applied Sciences, Himachal Pradesh Technical University, Hamirpur-177001, H.P., India.
* Corresponding author:
bspatial@gmail.com
bspatial@hpuniv.ac.in

sources/lasers, microstructure realization in integrated optics, the production of cost-effective solar cells and their emerging role as optical recorders utilizing reversible phase-change out of which the technological applications of threshold and memory switching are widely regarded as highly significant (Zakery & Elliott, 2003; Ovshinsky, 1968; Mott, 1971; Carlson & Wronski, 1976; Jiang & Okuda, 1991). In addition to nonlinear characteristics, there are pronounced features such as high transparency in the extensive middle and far-infrared spectral regions (Cui *et al.*, 2013), low melting point, low thermal conductivity and exceptional stability, enabling the creation of doped glasses with a variety of other elements (Yoon *et al.*, 2006; Lu *et al.*, 2013). While Se-based chalcogenide glasses have numerous applications, their major drawback is susceptibility to thermal instability. The addition of tellurium helps in overcoming this issue as well as the challenges associated with the limited durability due to susceptibility to corrosion and limited sensitivity exhibited by amorphous selenium (Chiba & Funakoshi, 1988; Patial *et al.*, 2013; Muragi *et al.*, 1988). Tellurium provides vital characteristics necessary for modern cutting-edge technologies that depend on chalcogen-based glasses (Wilhelm *et al.*, 2007). Common characteristics often encompass features such as far infra-red transmittance, crucial for applications in optical fiber and infrared optics (Zakery & Elliott, 2003; Raoux *et al.*, 2010) and rapid crystallization essential for phase change optical data storage devices (Wuttig & Steimer, 2007; Wuttig & Yamada, 2007; Wojciech *et al.*, 2007). The incorporation of a third component such as In into the Se-Te binary chalcogenide system results in the formation of stable glassy alloys. In conjunction with broadening the glass-forming region, there is a simultaneous generation of disorder in composition and configuration within the system (Patial *et al.*, 2011). The inclusion of a third element has been noted to contribute to the formation of a cross-linked structure, leading to a subsequent elevation in the glass transition of a material from a glassy state and the temperature at which the binary alloy undergoes crystallization. The presence of a metallic impurity such as Pb heightens the overall thermal stability of the Se-Te-In glassy system and also leads to an increase in conductivity. It also increases the conduction transition from *p*-type to *n*-type (Kastner *et al.*, 1976; Pattanaik & Srinivasan, 2003; Murugavel & Asokan, 1998; Tohge *et al.*, 1987). Thus, these are excellent for substituting the traditional *p-n* junction, making them optimal materials for such a replacement. Chalcogenide materials with the addition of Pb have garnered interest for a range of applications, including optical communication, high-resolution spectroscopy, analysis of optical fibers, as well as the detection of airborne contaminants like hydrocarbons in the atmosphere and swift analysis of vehicle emissions, thus positioning them as an enticing field for additional investigation (Tacke, 1995; Agne *et al.*, 1994; Anjali *et al.*, 2020; Patial *et al.*, 2022).

Studying the thermodynamic properties of chalcogenides is crucial in material science for gaining a profound insight into the fundamental process of transforming an amorphous system into a stable crystalline system. Differential scanning calorimetry (DSC) or Differential thermal analysis (DTA) stands out as the most extensively employed among standard thermal analysis techniques due to its ease of execution, high sensitivity, non-destructive nature and minimal sample requirements. One can investigate the kinetics of glass transformation through both isothermal and non-isothermal measurements (Patial *et al.*, 2011; Abu-Sehly, 2009; Abdel-Rahim *et al.*, 2005; Patial *et al.*, 2017; Imran *et al.*, 2001; Patial *et al.*, 2011) (Tripathi *et al.*, 2012; Deepika *et al.*, 2009). In the isothermal technique, the sample is rapidly heated to a temperature surpassing the glass transition temperature (T_g), and the heat generated during the subsequent crystallization process is continuously recorded as a function of time (t) at a constant temperature. In the non-isothermal approach, the sample undergoes heating, typically at a constant rate, generally starting from room temperature, and the resulting heat release is recorded as a function of either time or temperature. One drawback associated with the isothermal method is the inability to instantly achieve the desired test temperature. Furthermore, during the time required for the system to stabilize, measurements cannot be conducted. On the other hand, the non-isothermal method does not have this drawback (Starink & Zahra, 1997). Thus, for these mentioned reasons, non-isothermal technique has also been employed in the current study to investigate the amorphous-crystallization transformation kinetics in $Se_{79-x}Te_{15}In_6Pb_x$ (x = 0, 1, 2, 4, 6, 8 and 10) glassy alloys.

In the study previously from our lab, these samples were analyzed for structural, optical, dielectric and thermal study. In the thermal study, crystallization activation energy E_c was also deduced at

 https://doi.org/10.37819/nanofab.009.2020

peak temperature for each investigated alloy by different formulations assuming the constancy of E_c throughout the amorphous-crystallization process. The previous reports from our lab and other studies suggested that consideration of constant E_c is not apposite which motivate us to analyze the variations in activation energy of amorphous to crystalline phase transition of the samples $Se_{79-x}Te_{15}In_6Pb_x$ (x = 0, 1, 2, 4, 6, 8 and 10) under study. Many researchers got attracted to various applications derived from the phase transition of these materials from amorphous to crystalline (Kumar *et al.*, 2011; Tripathi, 2010; Shaaban & Tomsah, 2011).

In technological contexts, the thermal stability of chalcogenide glasses holds fundamental significance, as the range of viable operating temperatures is contingent upon the structural alterations and potential crystallization processes that occur at the given operational temperature. Therefore, the significance of the activation energy as a crucial parameter becomes more pronounced as it signifies the glass's thermal stability, and its magnitude mirrors the characteristics of a-c transformation. Within the Johnson-Mehl-Avrami (JMA) model framework, the Avrami exponent and E_c are constant during the crystallization process (Lopes *et al.*, 2014). Recent advancements in this area have revealed that these do not remain constant but exhibit fluctuations at different stages of transformation (Abu-Sehly, 2009; Abdel-Rahim *et al.*, 2005; Patial *et al.*, 2017; Liu *et al.*, 2004; Sahay & Krishnan, 2004; Joraid, 2005; Abu-Sehly & Elabbar, 2007). The idea of the variable activation energy effectively within a-c transformation during the crystallization process is generally determined by nucleation and growth which are likely to have different activation energies (Vyazovkin, 2000; Vyazovkin, 2000; Vyazovkin, 2000; Vyazovkin, 2003). It is pointed out that the correlation between activation energy variation and the degree of crystallization, and consequently temperature, can offer valuable insights into the diverse mechanisms involved in the transformation process (Vyazovkin, 2000). For the current investigation, the effective energy required to initiate the transition from a-c phase for $Se_{79-x}Te_{15}In_6Pb_x$ (x = 0, 1, 2, 4, 6, 8 and 10) chalcogenide glasses is determined using four iso-conversional methods namely KAS method (Kissinger, 1956; Kissinger, 1957; Akahira, 1971), OFW method (Ozawa, 1965; Flynn & Wall, 1966), Tang & Chen method (Wanjun & Donghua, 2005) and Starink method (Starink, 2003) to investigate the variation with degree of crystallization and temperature. These iso-conversional methods are incorporated into a Python code developed for this study, and all analyses are performed computationally which increases the reliability of the results and enhances their accuracy when concluding.

MATERIALS AND METHODS

Synthesis and DSC of $Se_{79-x}Te_{15}In_6Pb_x$

Glassy alloys composed of $Se_{79-x}Te_{15}In_6Pb_x$ (x = 0, 1, 2, 4, 6, 8, and 10) were synthesized through the melt quenching method. Materials with high purity (99.999%) of 5N are measured based on their atomic percentages and sealed in a quartz ampoule (length ~5 cm, diameter ~12 mm) under a vacuum of 2×10^{-5} mbar. The sealed ampoule was heated in a muffle furnace for 10 hours at the rate of 2-3°C/min up to 900°C. The ampoule was regularly agitated to ensure uniformity. The quenching is done in the chilled water rapidly. Thus, prepared bulk samples were ground into a fine powder for further analysis.

The nano-crystalline nature is identified by X-ray diffraction (XRD) and further confirmed by field emission scanning electron microscope (FESEM) (Anjali *et al.*, 2023). X-ray diffraction of investigated composition is performed at room temperature by taking XRD pattern of the examined samples through PANalytical X'Pert x-ray diffractometer in $10° < 2\theta < 90°$ range at 1°/min scanning rate using Cu $K\alpha$ (λ = 1.54056 Å). The investigation of premier characteristic peaks in the XRD spectrum signifies the nano nature of examined alloys. The surface morphology as well as the nanocrystalline nature of examined system is further analyzed by FESEM (HITACHI-SU8010) operating at an accelerating voltage of 15 kV; which indicates good consistency with XRD outcome.

The thermal data of the glasses under investigation is collected using Mettler Toledo *Star*^{e} DSC system under non-isothermal conditions for four different heating rates of 5, 10, 15 and 20 K/min. This equipment has a temperature accuracy of ±0.1°C. A standard alumina pan was used to seal a sample weighing 3-5 mg which was then subjected to heating in a dry nitrogen environment with non-isothermal conditions at a rate of 40 milliliters per minute in the range 30-500°C to investigate a-c transformation region. **Fig. 1** shows the DSC traces for all the samples $Se_{79-x}Te_{15}In_6Pb_x$ (x = 0, 1, 2, 4, 6, 8, and 10) under investigation at the heating rate 20°C/min. It can be seen from these curves

that well-defined glass transition region (first endothermic peak), crystallization region (exothermic peak) and melting (second endothermic peak) were observed. Similar traces were also observed for all the examined samples at other heating rates viz 5, 10 and 15°C/min (not shown here).

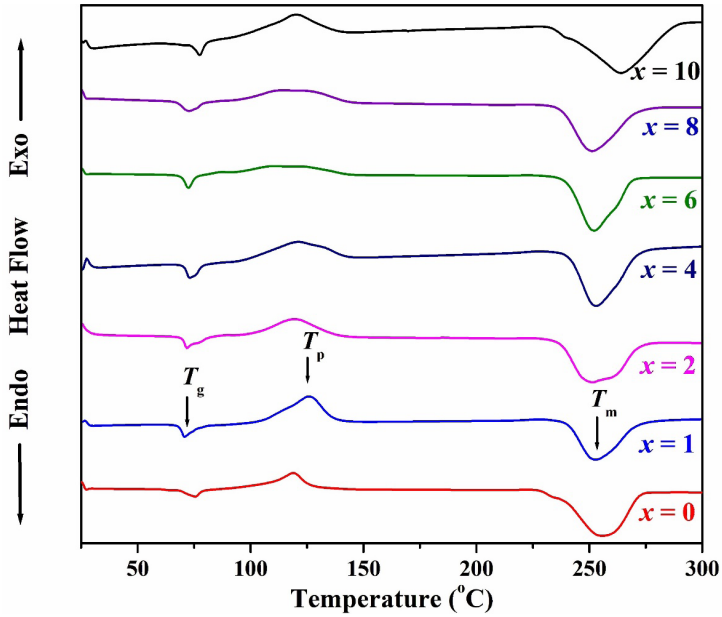

Figure 1. DSC curves for $Se_{79-x}Te_{15}In_6Pb_x$ (x = 0, 1, 2, 4, 6, 8, and 10) alloys at the heating rate 20°C/min.

Custom Python Code for Data Analysis

In this study, a Python code-named "HPU-B-MASS" was specifically developed for the analysis of data, calculations, and generation of the graphs. Sublime Text 3 was utilized as the integrated development environment for creating and refining this code, offering a streamlined and efficient platform for development. In this Python code, several essential features have been implemented that allow to accomplish a variety of tasks seamlessly. The code begins by importing the necessary libraries, such as numpy, pandas, scipy and matplotlib, ensuring access to a rich set of tools for data handling and analysis.

Firstly, the DSC-derived data on a-c transformation under non-isothermal conditions at four different heating rates α_i (5, 10, 15 & 20 K/min) is analyzed using this Python code. When the Python code is executed, it prompts the user to input the Excel file name, including the '.xlsx' extension, which contains the data obtained by DSC of $Se_{79-x}Te_{15}In_6Pb_x$ (x = 0, 1, 2, 4, 6, 8, and 10). The data includes temperature and heat flow values for each of the four different heating rates α_i (5, 10, 15 & 20 K/min). The Python code then automatically reads the data from the Excel file and stores it in arrays within the code for further calculations. Sub-intervals for interpolation are entered, using which temperature and heat flow values are interpolated. The Python code utilizes the Cubic Spline function from the SciPy library to perform interpolation, ensuring smooth transitions between data points. Matplotlib is used to generate graphs illustrating the relationship between temperature and heat flow for each heating rate. The code then proceeds to calculate the area under the curve using the interpolated points for each heating rate α_i (5, 10, 15 & 20 K/min). For loop is implemented to calculate the area under the curve using the two-point trapezoidal rule for each segment. Along with the two-point trapezoidal rule, Simpson's 1/3rd rule is also incorporated to compare the accuracy and results of each method. For the two-point trapezoidal rule, the area under the curve is calculated by taking two of the n interpolated points at a time and applying the rule. For a given number of interpolated points, the algorithm starts by calculating the area of the first trapezoid under the curve and storing it in the variable 'total area'. It then computes the area of the next trapezoid and adds it to the current value of 'total area'. This process continues until the area for the nth trapezoid is calculated, with each result being

added to 'total area'. Consequently, the final value of 'total area' represents the cumulative area under the curve. Linear curve fitting or regression analysis is employed in the Python code to establish a linear relationship between the variables *x* and *y*. This technique is utilized to determine the optimal fit for the data, resulting in a precise representation of the results. The calculations performed in this research provide an accuracy of up to two decimal points. This precision can be easily increased by adjusting the number of interpolation points accordingly.

RESULTS AND DISCUSSION

The variation of heat flow versus temperature for a-c transformation in $Se_{79}Te_{15}In_6$ at all four heating rates is shown in **Fig. 2.** The similar variation was also observed for other investigated samples (not shown here). The extent of crystallization (χ) was assessed utilizing the partial area technique. The determination of the crystallized fraction (χ) at a given temperature (T) involves the calculation $\chi = A_T/A$, where A represents the total area under the exothermic peak occurring between the initial temperature (T_i), marking the onset of crystallization, and the final temperature (T_f), indicating complete crystallization. The term A_T denotes the area under the peak between temperatures T_i and T. **Fig. 3** shows the crystallization fraction at a generic temperature T (shaded area of exothermic peak). The relationship between temperature and the crystallized fraction follows a sigmoid curve, as depicted in the literature (Abu-Sehly & Elabbar, 2007; Shaaban *et al.*, 2009).

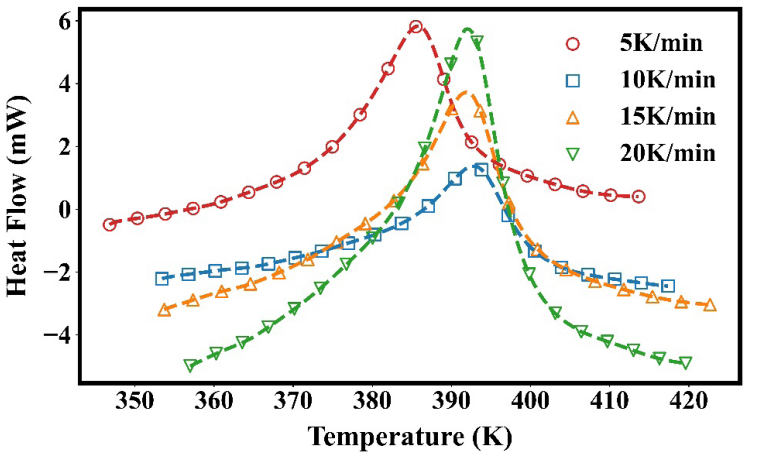

Figure 2. Heat flow versus temperature for crystallization peaks in $Se_{79}Te_{15}In_6$ at heating rates 5, 10, 15 and 20 K/min.

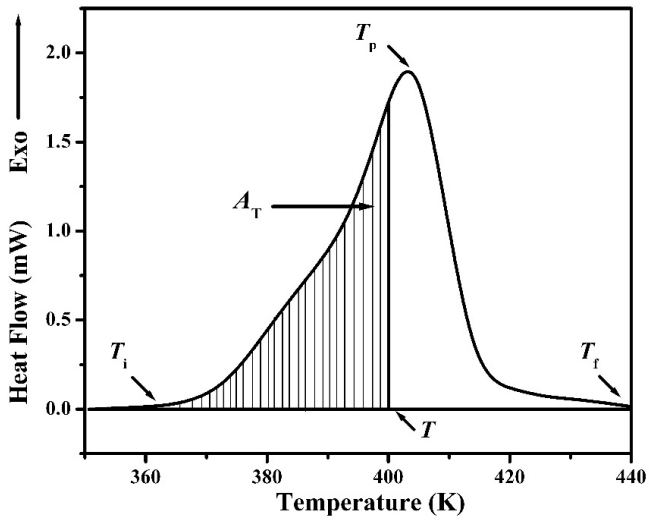

Figure 3. Crystallization fraction at a generic temperature *T*.

A sigmoid curve typically has an S-shaped appearance, starting slowly, increasing steeply in the middle, and then leveling off. It is observed that all the examined samples show almost similar type sigmoid curves (**Fig. 4**) in the entire range of the considered temperatures. **Fig. 4** shows the aforementioned variation for Pb additive samples; $Se_{78}Te_{15}In_6Pb_1$, $Se_{77}Te_{15}In_6Pb_2$, $Se_{75}Te_{15}In_6Pb_4$, $Se_{73}Te_{15}In_6Pb_6$, $Se_{71}Te_{15}In_6Pb_8$ and $Se_{69}Te_{15}In_6Pb_{10}$ at four heating rates; 5, 10, 15 and 20 K/min. The sigmoid curve here suggests a temperature range over which crystallization is initiated and then proceeds to completion. The steep ascent in the middle of the curve represents the phase where crystallization accelerates and the leveling off indicates that the crystallization process is nearly completed at higher temperatures. The plotted experimental data is presented in **Fig. 4** and using this data, the code determines the corresponding temperature for crystallization fractions χ = 0.1, 0.2, 0.3, 0.4, 0.5, 0.6, 0.7, 0.8 and 0.9. These temperature values are used to compute the *x*- and *y*-coordinates for generating graphs in all four iso-conversional methods; KAS, OFW, Tang & Chen, and the Starink methods.

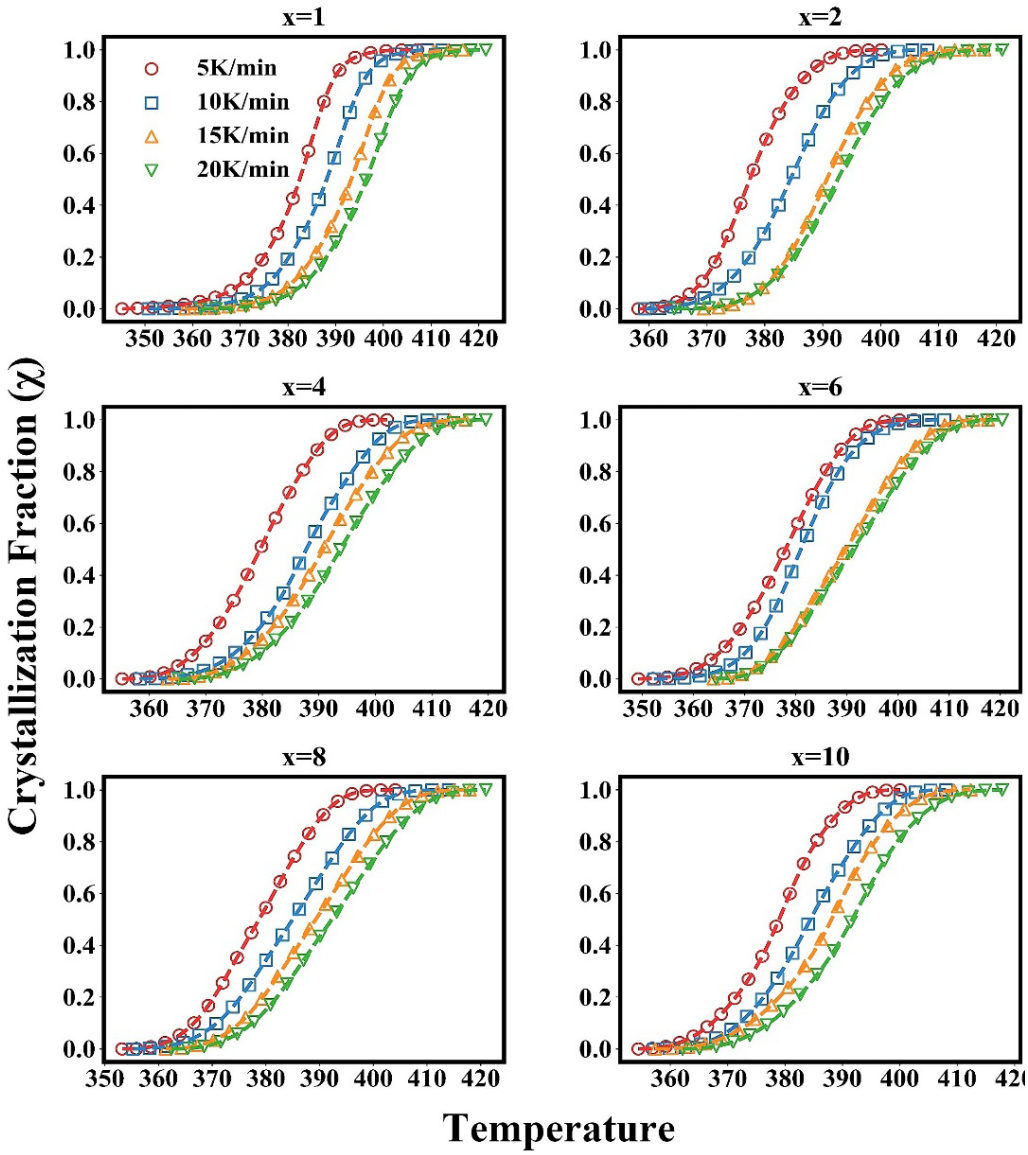

Figure 4. Variation of crystallized fraction as a function of temperature for $Se_{78}Te_{15}In_6Pb_1$, $Se_{77}Te_{15}In_6Pb_2$, $Se_{75}Te_{15}In_6Pb_4$, $Se_{73}Te_{15}In_6Pb_6$, $Se_{71}Te_{15}In_6Pb_8$ and $Se_{69}Te_{15}In_6Pb_{10}$ at four heating rates; 5, 10, 15 and 20 K/min.

 https://doi.org/10.37819/nanofab.009.2020

The KAS (Kissinger, 1956; Kissinger, 1957; Akahira, 1971) method is based on the equation given below:

$$\ln\left(\frac{\alpha_i}{T_{\chi_i}^2}\right) = -\frac{E_{\chi_i}}{RT_{\chi_i}} + constant \quad (1)$$

This equation allows for the determination of the activation energy $E_{\chi i}$ without needing to assume a specific reaction model. It involves measuring the temperatures at the different heating rates α_i and plotting $\ln(\alpha_i/T_{\chi i}^2)$ versus $1000/T_{\chi i}$ to obtain the slope, which is proportional to the activation energy i.e. activation energy at each degree of conversion can be calculated.

The OFW (Ozawa, 1965; Flynn & Wall, 1966) method considers the heating rate only on the left-hand side and the deduced expression is:

$$\ln(\alpha_i) = -\frac{1.0516E_{\chi_i}}{RT_{\chi_i}} + constant \quad (2)$$

This method focuses on how the heating rate influences the conversion rate. It does not require knowledge of the reaction order, making it useful for various materials and processes. Plotting of $(\ln\alpha_i)$ versus $1000/T_{\chi i}$ is used to deduce the slope and hence activation energy.

The expression for the Tang and Chen method (Wanjun & Donghua, 2005) is given by:

$$\ln\left(\frac{\alpha_i}{T_{\chi_i}^{1.895}}\right) = -\frac{1.00145\,E_{\chi_i}}{RT_{\chi_i}} + constant \quad (3)$$

This method refines the estimation of the activation energy by introducing a factor for the temperature dependence in the denominator. The equation is used to evaluate kinetic parameters by accounting for slight variations in temperature power thus allowing a more precise calculation of the activation energy than KAS method. Thus, in this method, the variation of $\ln(\alpha_i/T_{\chi i}^{1.895})$versus $1000/T_{\chi i}$ is used to derive $E_{\chi i}$.

The relationship used in the Starink (Starink, 2003) method is as follows:

$$\ln\left(\frac{\alpha_i}{T_{\chi_i}^{1.92}}\right) = -\frac{1.0008E_{\chi_i}}{RT_{\chi_i}} + constant \quad (4)$$

This method is similar to the Tang & Chen method but with a different temperature exponent. The equation suggests a refined approximation for kinetic studies. This method provides a reliable estimation of activation energy by slightly modifying the temperature exponent, improving accuracy in various kinetic analyses.

In the given context, the subscript *i* denotes the different heating rates (5, 10, 15 & 20 K/min), *R* is the universal gas constant (8.314 $JK^{-1}mol^{-1}$), $E_{\chi i}$ and $T_{\chi i}$ denotes the activation energy (E_c) and temperature (T) in more generalized manner for each χ respectively. A corresponding $T_{\chi i}$ and heating rate α_i for each degree of the conversion χ are used to calculate the values of $\ln(\alpha_i/T_{\chi i}^2)$ for KAS, $(\ln\alpha_i)$ for OFW, $\ln(\alpha_i/T_{\chi i}^{1.895})$ for Tang and Chen and $(\ln\alpha_i/T_{\chi i}^{1.92})$ for Starink method using the code. Each of these values is plotted against $1000/T_{\chi i}$ to obtain four different graphs

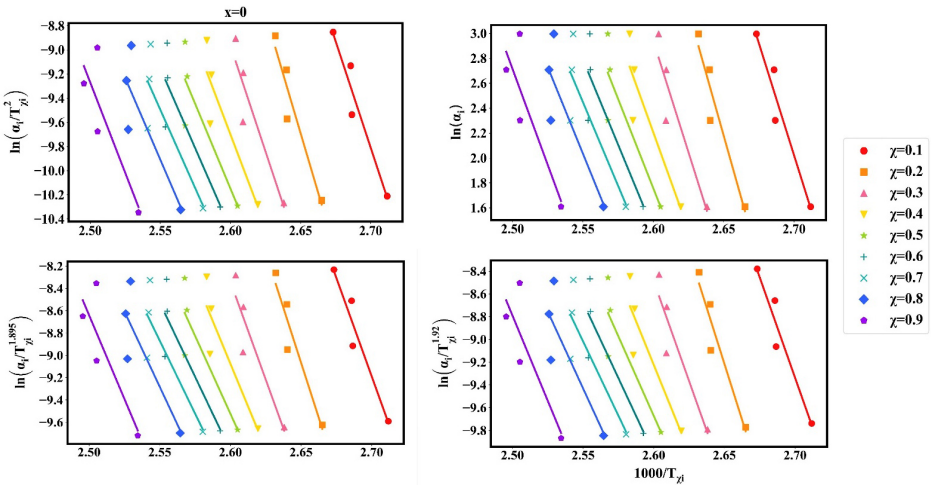

Figure 5. Plot of $\ln(\alpha_i/T_{\chi i}^2)$ versus $1000/T_{\chi i}$ obtained using KAS method, $(\ln\alpha_i)$ versus $1000/T_{\chi i}$ obtained using OFW method, $\ln(\alpha_i/T_{\chi i}^{1.895})$ versus $1000/T_{\chi i}$ obtained using Tang & Chen method, $\ln(\alpha_i/T_{\chi i}^{1.92})$ versus $1000/T_{\chi i}$ obtained using Starink method, for $Se_{79}Te_{15}In_6$.

for each iso-conversional method concerning the crystallized fraction, $\chi = 0.1 - 0.9$. The plot appears as a straight line, as shown in **Fig. 5** with the slopes calculated using the code. Further, **Fig. 6** depicts the determination of E_c concerning the crystallized fraction, $\chi = 0.1 - 0.9$ for the glassy alloy with the composition $Se_{79}Te_{15}In_6$ using the KAS, OFW, Tang & Chen, and Starink methods. A similar procedure is also opted for the determination of the E_c in the other samples. The slope values are pivotal in enabling the code to deduce the activation energy corresponding to each χ value. The plot of KAS gives the slope $-E_\chi/R$, OFW gives the slope −1.0516 E_χ/R, Tang & Chen gives the slope −1.00145 E_χ/R and Starink method gives the slope −1.0008 E_χ/R from which the code calculates the values of activation energy for each iso-conversional method. The calculated activation energy values are then printed in the form of the table by the Python code. These values are given in **Tables 1, 2, 3** and **4.**

	E_c						
χ	$x = 0$	$x = 1$	$x = 2$	$x = 4$	$x = 6$	$x = 8$	$x = 10$
0.1	293.02	115.80	112.30	131.68	119.76	137.37	157.74
0.2	237.11	118.86	108.85	124.14	123.27	131.17	147.33
0.3	291.59	118.74	105.67	120.37	118.78	127.55	140.20
0.4	254.44	117.99	103.16	117.28	110.79	123.51	133.90
0.5	231.97	116.83	100.68	115.38	101.74	120.36	129.49
0.6	220.93	115.48	98.98	112.78	94.59	116.67	126.65
0.7	216.90	114.01	97.80	110.37	90.16	112.85	124.26
0.8	224.51	112.26	96.93	107.34	86.65	110.58	121.85
0.9	249.81	110.06	95.82	103.98	83.96	106.44	118.50

Table 1. Values of E_c (kJmol^{-1}) for $Se_{79-x}Te_{15}In_6Pb_x$ at $\chi = 0.1 - 0.9$ by KAS method.

	E_c						
χ	$x = 0$	$x = 1$	$x = 2$	$x = 4$	$x = 6$	$x = 8$	$x = 10$
0.1	284.51	116.08	112.72	131.12	119.76	136.51	155.88
0.2	317.02	119.06	109.49	124.02	123.15	130.68	146.06
0.3	283.31	118.99	106.51	120.49	118.94	127.29	139.33
0.4	248.03	118.32	104.16	117359	111.39	123.49	133.39
0.5	226.70	117.26	101.82	115.83	102.83	120.54	129.23
0.6	216.24	116.00	100.24	113.40	96.08	117.08	126.56
0.7	212.43	114.63	99.15	111.14	91.91	113.50	124.32
0.8	219.70	112.99	98.37	108.31	88.62	11.39	122.08
0.9	243.83	110.95	97.37	105.18	86.13	107.52	118.95

Table 2. Values of E_c (kJmol^{-1}) for $Se_{79-x}Te_{15}In_6Pb_x$ at $\chi = 0.1 - 0.9$ by OFW method.

Fig. 6 shows the correlation between the extent of conversion (χ) and activation energy (E_c) along with its correlation to the temperature (T) for different iso-conversional methods. The values of E_c and T used is calculated for each corresponding degree of the conversion χ (0.1 − 0.9). The correlation between the activation energy and the extent of conversion is represented by the points and that between temperature and extent of conversion is shown by the solid lines. Even though there is a spike in the value of E_c with χ at first, the general trend is a decrease in the value of E_c for all four iso-conversional methods. Similar plots are also observed for all other investigated samples. The bold points (see **Fig. 6**) show the correlation between the extent of transformation and E_c, for crystallization region for the investigated $Se_{79}Te_{15}In_6$ alloy. Similar variations are also observed for the other investigated samples. The data presented in the tables demonstrate a significant fluctuation in the local apparent activation energy concerning the extent of transformation across all four a-c transformations methods. Across these methods, a consistent trend emerges a progressive reduction in the activation energy at the local level as the χ increases. Notably, it is important to highlight the good agreement observed

among the KAS, OFW, Tang & Chen, and Starink methods. Furthermore, the variation in **Fig. 6** also depicts the correlation between the temperature and the resultant local activation energy for crystallization (E_c). The variation in E_c with temperature is accomplished by replacing the degree of crystallization with a determined mean temperature associated with that particular degree of crystallization at various heating rates (Vyazovkin & Dranca, 2006). The estimated average temperature is also computed using the code. The solid line in the figure indicates that as the temperature increases during the crystallization process, there is an expected corresponding rise in the magnitude of crystallized fraction χ.

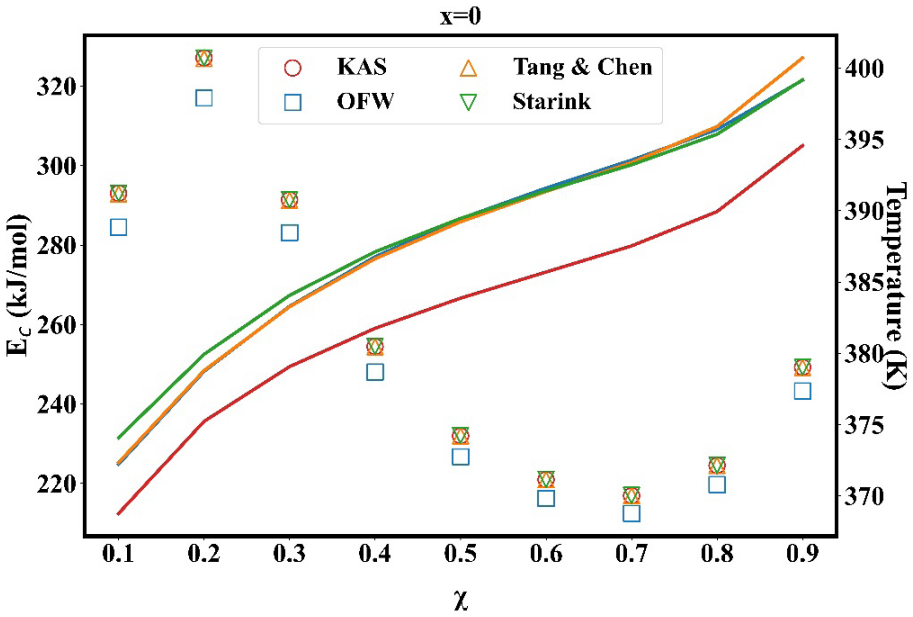

Figure 6. The relationship between the local activation energy with χ and temperature as identified through four iso-conversional methods for $Se_{79}Te_{15}In_6$.

Each of the four iso-conversational methods shows a reduction in the E_c with rising temperature, suggesting an augmentation in the crystallization rate as the temperature increases. Hence, it becomes apparent that the a-c transformation is best explained by a series of intricate multi-step reactions, encompassing various growth processes. Instead of a single-step mechanism, there are varying activation energies and mechanisms involved. The decrease in activation energy with increasing temperature supports the notion that both nucleation and growth processes jointly govern the crystallization rate constant. This aligns with the conclusions drawn by other researchers (Kumar *et al.*, 2009; Kaur *et al.*, 2000; Maharjan *et al.*, 2003).

	E_c						
χ	x = 0	x = 1	x = 2	x = 4	x = 6	x = 8	x = 10
0.1	292.92	115.97	112.47	131.81	119.91	137.49	157.83
0.2	326.96	119.02	109.02	124.29	123.41	131.30	147.44
0.3	291.50	118.90	105.85	120.53	118.94	127.70	140.32
0.4	254.50	118.16	103.35	117.44	110.96	123.66	134.04
0.5	231.97	117.00	100.86	115.55	101.93	120.52	129.64
0.6	220.95	115.66	99.18	112.96	94.79	116.84	126.80
0.7	216.93	114.18	98.00	110.55	90.37	113.03	124.41
0.8	224.53	112.44	97.13	107.53	86.86	110.77	122.02
0.9	249.79	110.25	96.03	104.18	84.18	106.63	118.68

Table 3. Values of E_c (kJmol^{-1}) for $Se_{79-x}Te_{15}In_6Pb_x$ at χ = 0.1 – 0.9 by Tang & Chen method.

	E_c						
χ	$x = 0$	$x = 1$	$x = 2$	$x = 4$	$x = 6$	$x = 8$	$x = 10$
0.1	293.03	115.96	112.46	131.82	119.92	137.50	157.86
0.2	327.10	119.02	109.01	124.29	123.42	131.31	147.46
0.3	291.61	118.90	105.84	120.53	118.94	127.70	140.34
0.4	254.49	118.15	103.33	117.44	110.96	123.66	134.05
0.5	232.04	117.00	100.85	115.55	101.92	120.52	129.64
0.6	221.01	115.65	99.16	112.95	94.77	116.83	126.81
0.7	216.99	114.18	97.98	110.54	90.35	113.02	124.41
0.8	224.59	112.43	97.12	107.51	86.84	110.76	122.02
0.9	249.87	110.24	96.01	104.17	84.16	106.62	118.67

Table 4. Values of E_c (kJmol^{-1}) for $Se_{79-x}Te_{15}In_6Pb_x$ at χ = 0.1 – 0.9 by Starink method.

Thermal reactions often involve multiple steps and complex mechanisms that change at different degrees of conversion. Some methods are more sensitive to these changes than others. For example, the OFW method can sometimes overestimate activation energies at higher conversion rates due to its mathematical nature. Thus, the sensitivity of each method to changes in reaction mechanism influences the variations in E_c values at different conversion levels. While comparing these methods, the KAS method fits well because of its direct integration approach as it minimizes errors associated with complex approximations, leading to more accurate and reliable estimates of activation energy, especially at different degrees of conversion. Along with it, this method also comes with adaptability to changes in reaction mechanisms, robustness to experimental variations and effectiveness in dealing with multi-step reactions. These characteristics make it a reliable method for determining activation energy across different degrees of conversion. Also, the Starink method often provides more consistent and reliable values of activation energy across different degrees of conversion because it minimizes the approximation errors seen in other methods. Here, the logarithmic relationship between the heating rate and a temperature-dependent term ($T^{1.92}$) is plotted against $1/T$ and the slope provides a more accurate estimate of the activation energy. Therefore, by introducing a correction term ($T^{1.92}$) in the equation, this method provides a better fit, especially when dealing with complex reactions and multi-step processes. Also, it is generally more robust against experimental variations due to its modified mathematical treatment. In general, if the reaction involves complex mechanisms or significant variations in activation energy across different degrees of conversion, the Starink method is preferable. However, for simpler reactions or when a straightforward analysis is desired, the KAS method is adequate.

The activation energy for these two mechanisms typically differs and hence causes the effective activation energy to change in response to temperature fluctuations (Vyazovkin, 2000). The foundation of this comprehension lies in the nucleation theory introduced by Fisher and Turnbull (Turnbull & Fisher, 1949), which posits that the relationship between the crystallization rate, denoted as *r*, and temperature dependence is expressed as:

$$r = r_0 \exp\left(-\frac{E_D}{RT}\right) \exp\left(-\frac{\Delta F}{k_B T}\right) \quad (5)$$

In the above equation, *r* describes how quickly the material transitions from an amorphous (or glassy) state to a crystalline state. This rate depends on various factors, including temperature, activation energy and nucleation dynamics. r_0 represents a pre-exponential factor related to the intrinsic properties of the material and the crystallization process. It represents the crystallization rate under ideal conditions without energy barriers. E_D denotes the activation energy for atomic or molecular diffusion, k_B stands for the Boltzmann constant which relates the energy at the atomic or molecular scale to temperature. Additionally, ΔF signifies the free energy change required to form a critical nucleus of the new crystalline phase. It is a key factor in nucleation theory because it dictates how readily a new phase (like a crystal) can form within the existing material. A higher ΔF indicates a more challenging nucleation process.

The equation consists of two exponential terms, each addressing different aspects of the crystallization process. The first exponential term ($\exp(-E_D/RT)$) describes how the crystallization rate is influenced by the activation energy for diffusion (E_D) and temperature. A higher E_D means that more energy is required for atoms to move and form an ordered crystal structure. As temperature increases, the exponential term becomes larger (less negative), which enhances the rate of diffusion and consequently, the crystallization rate. The second exponential term ($\exp(-\Delta F/(k_B T))$) is related to the nucleation process, where ΔF represents the free energy change required to form a stable nucleus of the new phase. The probability of forming such a nucleus increases as temperature rises, as indicated by the dependence on T in the denominator. A higher temperature reduces the value of $\Delta F/(k_B T)$, making the exponential less negative, which increases the crystallization rate. The equation suggests that the crystallization rate (r) is primarily governed by two factors: atomic diffusion (via the first exponential term) and nucleation (via the second exponential term).

Nucleation theory posits that a new phase (e.g., a crystal) forms through the creation of small clusters (nuclei) of atoms. For crystallization to occur, these nuclei must overcome an energy barrier (ΔF), after which the formation of the crystalline structure can proceed rapidly. The reduction in the activation energy of crystallization (E_c) can be linked to changes in these parameters, such as temperature or material composition, which affect how readily atoms can move and nucleate a new phase.

Compositional Dependence of E_c

It can be seen from Tables 1-4 that the values of E_c obtained for the investigated alloys from different methods are different. This difference can be attributed to the fact that these methods are based on approximations involved in obtaining the final equation of different formalisms. Furthermore, our findings suggest an increased propensity for crystallization in glasses with Pb content leading to an observed reduction in crystallization activation energy i.e., Pb-additive samples have lower activation energy as compared to the parent ternary alloy. Further, there is a slight variation in the value of E_c deduced from different methods for each degree of conversion (Tables 1-4). This variation may be arising due to various assumptions taken during their formulations. On comparing deduced E_c values through different empirical routes; it is concluded that either of these formulations can also be utilized to realize E_c value at a particular extent of conversion along with distinct precisions. The derived values of E_c of these samples at different degrees of conversion are in concordance with the observed values of activation energy of crystallization for the alloys analyzed previously from our lab.

Understanding the variable activation energy helps in the precise control and optimization of the crystallization process in chalcogenide glasses, which are used in various applications including optical devices and electronic components. The study's findings can improve predictive models for the thermal behavior of similar materials, aiding in the development of more reliable materials for industrial applications. Enhanced knowledge of activation energy variations supports better quality control in the manufacturing of chalcogenide glasses, ensuring consistent performance in their applications.

CONCLUSIONS

In the present study, the chalcogenide glassy alloys of the composition under study are prepared by melt quenching technique. The kinetics of the phase transformation from amorphous-crystallization (a-c) transition in thus primed chalcogenide glassy alloys are investigated using DSC technique under non-isothermal conditions. The iso-conversational analysis of a-c transformation is conducted. The entire process, including calculations, graph generation, and table creation, was carried out computationally using Python code-named '*HPU-B-MASS*'. The indications provided by the crystallization activation energy values (E_c) demonstrate a consistent agreement and a comparable pattern of variation in E_c is evident with both the degree of conversion χ and temperature T across all four iso- conversional methods. Upon reheating the chalcogenide material, the nuclei converge leading to the formation of a novel and intricate phase through nucleation. Concurrently, the new phase undergoes growth. By considering the distinct activation energies governing the nucleation and growth processes in the a-c transformation, it can be anticipated that there is a temperature-dependent fluctuation in the effective crystallized activation energy. This phenomenon aligns with the principles outlined in Turnbull and Fisher's theory. The present investigation discloses that the shift from amorphous to crystalline state in the analyzed samples entails an intricate procedure, marked

by diverse mechanisms of nucleation and growth. The activation energy, obtained through the four iso-conversional methods; the KAS, OFW, Tang & Chen, and Starink methods, is observed to change about both the degree of conversion χ and the temperature *T*. Each of the four iso-conversional methods indicated that the activation energy varies with the temperature. Therefore, computational iso-conversional analysis leads to the conclusion that assuming a constant value for E_c is inappropriate.

Thus, this study highlights the variable nature of activation energy in the investigated Se-Te-In-Pb chalcogenide system, demonstrating that activation energy changes with both degrees of conversion as well as temperature. The findings challenge the assumption of constant activation energy, emphasizing the need for accurate iso-conversional analysis to better understand the crystallization behavior of these materials. Thus, future research can apply the iso-conversional analysis to other types of glasses and materials to explore if similar variations in activation energy occur, potentially leading to new insights in material science. The Python algorithm used in this study can be further developed and adapted for analyzing other complex thermal processes, enhancing the tools available for researchers in the field. The study's results can contribute to the refinement of theoretical models for crystallization and phase transitions, potentially leading to advancements in material design and processing.

Conflict of Interest

The authors affirm that this research was carried out without any financial or commercial affiliations that could be viewed as a potential conflict of interest. ♦

REFERENCES

Abdel-Rahim, M. A., Hafiz, M. M., & Shamekh, A. M. (2005). A study of crystallization kinetics of some Ge-Se-In glasses. *Physica B: Condensed Matter, 369*, 143-154. https://doi.org/10.1016/j.physb.2005.08.007

Abu-Sehly, A. A. (2009). Variation of the activation energy of crystallization in $Se_{81.5}Te_{16}$ $Sb_{2.5}$ chalcogenide glass: Isoconversional analysis. *Thermochim. Acta, 485*, 14-19. https://doi.org/10.1016/j.tca.2008.12.006

Abu-Sehly, A. A., & Elabbar, A. A. (2007). Kinetics of crystallization in amorphous $Se_{73.2}Te_{21.1}$ $Sb_{5.7}$ under isochronal conditions: Effect of heating rate on the activation energy. *Physica B: Condensed Matter, 390*, 196-202. https://doi.org/10.1016/j.physb.2006.08.014

Agne, M., Lambrecht, A., Schiessl, U., & Tacke, M. (1994). Guided modes and far-field patterns of lead chalcogenide buried heterostructure laser diodes. *Infrared Physics & Technology, 35*, 47-58. https://doi.org/10.1016/1350-4495(94)90041-8

Akahira, T. (1971). Trans. Joint convention of four electrical institutes. *Res. Rep. Chiba Inst. Technol., 16*, 22-31. https://cir.nii.ac.jp/crid/1571417125949031680

Anjali, Patial, B. S., & Thakur, N. (2020). On the structural and thermophysical study of Pb-doped Se-Te-In nanochalcogenide alloys. *Journal of Asian Ceramic Societies, 8*, 777-792. https://doi.org/10.1080/21870764.2020.1789289

Anjali, Patial, B. S., Sharma, P., & Thakur, N. (2023). Pb-additive Se-Te-In nano-chalcogenide thin films: preparation, morphological, optical analysis and material perspective for phase-change memory devices. *Journal of Materials Science: Materials in Electronics, 34*, 1833. https://doi.org/10.1007/s10854-023-11164-5

Carlson, D. E., & Wronski, C. R. (1976). Amorphous silicon solar cell. *Applied Physics Letters, 28*, 671-673. https://doi.org/10.1063/1.88617

Chiba, R., & Funakoshi, N. (1988). Crystallization of vacuum deposited Te_{100-x} $Se_{x0.7}$ Cu_{30} alloy film. *Journal of Non-crystalline Solids, 105*, 149-154. https://doi.org/10.1016/0022-3093(88)90349-3

Cui, S., Chahal, R., Boussard-Plédel, C., Nazabal, V., Doualan, J.-L., Troles, J., … Bureau, B. (2013). From selenium-to tellurium-based glass optical fibers for infrared spectroscopies. *Molecules, 18*, 5373-5388. https://doi.org/10.3390/molecules18055373

Deepika, Rathore, K. S., & Saxena, N. S. (2009, July). A kinetic analysis on non-isothermal glass-crystal transformation in Ge_{1-x} Sn_x $Se_{2.5}$ ($0 \leq x \leq 0.5$) glasses. *Journal of Physics: Condensed Matter, 21*, 335102. https://doi.org/10.1088/0953-8984/21/33/335102

Flynn, J. H., & Wall, L. A. (1966). General treatment of the thermogravimetry of polymers. *Journal of research of the National Bureau of Standards. Section A, Physics and Chemistry, 70*, 487. https://doi.org/10.6028%2Fjres.070A.043

Imran, M., Bhandari, D., & Saxena, N. (2001). Kinetic studies of bulk Ge_{22} Se_{78-x} Bi_x (x = 0, 4 and 8) semiconducting glasses. *J. Therm.*

Anal. Calorim., *65*, 257-274. https://doi.org/10.1023/a:1011557425244

Jiang, F. J., & Okuda, M. O. (1991). The effect of doping on the erasure speed and stability of reversible phase-change optical recording films. *Japanese Journal of Applied Physics, 30*, 97. https://doi.org/10.1143/JJAP.30.97

Joraid, A. A. (2005). Limitation of the Johnson-Mehl-Avrami (JMA) formula for kinetic analysis of the crystallization of a chalcogenide glass. *Thermochim. Acta*, *436*, 78-82. https://doi.org/10.1016/j.tca.2005.07.005

Kastner, M., Adler, D., & Fritzsche, H. (1976). Valence-alternation model for localized gap states in lone-pair semiconductors. *Physical Review Letters, 37*, 1504. https://doi.org/10.1103/PhysRevLett.37.1504

Kaur, G., Komatsu, T., & Thangaraj, R. (2000). Crystallization kinetics of bulk amorphous Se-Te-Sn system. *Journal of Materials science, 35*, 903-906. https://doi.org/10.1023/A:1004798308059

Kissinger, H. E. (1956). Differential thermal analysis. *J. Res. Natl. Bur. Stand, 57*, 217. https://books.google.com/books?hl=en&lr=&id=AD5XTgl1T0wC&oi=fnd&pg=PA217&dq=+H.E.+Kissinger,+J+Res+Natl+Bur+Stand+57(1956)+217&ots=MW5nHDRyhj&sig=RZH2YLZrkKMJcuJHpxEW3ldYutQ

Kissinger, H. E. (1957). Reaction kinetics in differential thermal analysis. *Analytical Chemistry, 29*, 1702-1706. https://doi.org/10.1021/ac60131a045

Kumar, H., Mehta, N., & Kumar, A. (2011). Effect of some chemical modifiers on the glass/crystal transformation in binary Se_{90} In_{10} alloy. *J. Therm. Anal. Calorim., 103*, 903-909. https://doi.org/10.1007/s10973-010-1181-2

Kumar, H., Mehta, N., & Singh, K. (2009). Calorimetric studies of glass transition phenomenon in glassy Se_{80-x} Te_{20} Sn_x alloys. *Physica Scripta*, *80*, 065602. https://doi.org/10.1088/0031-8949/80/06/065602

Lankhorst, M. H., Ketelaars, B. W., & Wolters, R. A. (2005). Low-cost and nanoscale non-volatile memory concept for future silicon chips. *Nature Materials, 4*, 347-352. https://doi.org/10.1038/nmat1350

Liu, F., Sommer, F., & Mittemeijer, E. J. (2004). Determination of nucleation and growth mechanisms of the crystallization of amorphous alloys; application to calorimetric data. *Acta Materialia, 52*, 3207-3216. https://doi.org/10.1016/j.actamat.2004.03.020

Liu, Q., Gan, F., Zhao, X., Tanaka, K., Narazaki, A., & Hirao, K. (2001). Second-harmonic generation in Ge_{20} As_{25} S_{55} glass irradiated by an electron beam. *Optics Letters, 26*, 1347-1349. https://doi.org/10.1364/OL.26.001347

Lopes, A. A., Monteiro, R. C., Soares, R. S., Lima, M. M., & Fernandes, M. H. (2014). Crystallization kinetics of a barium-zinc borosilicate glass by a non-isothermal method. *J. Alloys and Compounds, 591*, 268-274. https://doi.org/10.1016/j.jallcom.2013.12.086

Lu, Y., Song, S., Shen, X., Wu, L., Song, Z., Liu, B., … Nie, Q. (2013). Investigation of $Ga_8Sb_{34}Se_{58}$ material for low-power phase change memory. *ECS Solid State Letters, 2*, P94. https://doi.org/10.1149/2.008310ssl

Maharjan, N. B., Singh, K., & Saxena, N. S. (2003). Calorimetric studies in $Se_{75}Te_{25-x}Sn_x$ chalcogenide glasses. *Physica Status Solidi (a), 195*, 305-310. https://doi.org/10.1002/pssa.200305918

Mott, N. F. (1971). Conduction in non-crystalline systems: VIII. The highly correlated electron gas in doped semiconductors and in vanadium monoxide. *Philosophical Magazine, 24*, 935-958. https://doi.org/10.1080/14786437108217059

Muragi, B. D., Zope, M. J., & Zope, J. K. (1988). Mechanism for nonlinear IV behaviour and the temperature dependence of threshold switching in the Se-Te-Sn system. *Applied Physics A, 46*, 299-303. https://doi.org/10.1007/BF01141596

Murugavel, S., & Asokan, S. (1998). Carrier-type reversal in Pb-modified chalcogenide glasses. *Physical Review B, 58*, 4449. https://doi.org/10.1103/PhysRevB.58.4449

Ovshinsky, S. R. (1968). Reversible electrical switching phenomena in disordered structures. *Phys. Rev. Lett., 21*, 1450. https://doi.org/10.1103/PhysRevLett.21.1450

Ozawa, T. (1965). A new method of analyzing thermogravimetric data. *Bulletin of the Chemical Society of Japan, 38*, 1881-1886. https://doi.org/10.1246/bcsj.38.1881

Patial, B. S., Sharma, N., Bhardwaj, S., & Thakur, N. (2022). Crystallization study of Pb additive Se-Te-Ge nanostructured alloys using non-isothermal differential scanning calorimetry. *Nanofabrication, 7*, 138-145. https://doi.org/10.37819/nanofab.007.195

Patial, B. S., Thakur, N., & Tripathi, S. K. (2011). Crystallization Study of Sn additive Se-Te Chalcogenide Alloys. *J. Therm. Anal. Calorim., 106*, 845.

Patial, B. S., Thakur, N., & Tripathi, S. K. (2011). On the crystallization kinetics of In additive Se-Te chalcogenide glasses. *Thermochim. Acta, 513*, 1-8. https://doi.org/10.1016/j.tca.2010.09.009

Patial, B. S., Thakur, N., & Tripathi, S. K. (2013). Kinetics of amorphous-crystallization transformation of $Se_{85-x}Te_{15}$ Sn_x (x= 2, 4 and 6) alloys under non-isothermal conditions using Matusita's approach. *AIP Conf. Proc., 1512*, pp. 542-543. https://doi.org/10.1063/1.4791151

Patial, B. S., Thakur, N., & Tripathi, S. K. (2011). Crystallization Study of Sn additive Se-Te Chalcogenide Alloys. *J. Therm. Anal. Calorim., 106*, 845-852. https://doi.org/10.1007/s10973-011-1579-5

Pattanaik, A. K., & Srinivasan, A. (2003). Electrical and optical properties of amorphous Pb_x In_{25-x} Se_{75} films with a dispersion of nanocrystallites. *Journal of Optoelectronics and Advanced Materials, 5*, 1161-1167. https://old.joam.inoe.ro/arhiva/pdf5_5/Pattanaik.pdf

Raoux, S., Wełnic, W., & Ielmini, D. (2010). Phase change materials and their application to nonvolatile memories. *Chemical Reviews, 110*, 240-267. https://doi.org/10.1021/cr900040x

Sahay, S. S., & Krishnan, K. (2004). Modeling the isochronal crystallization kinetics. *Physica B: Condensed Matter, 348*, 310-316. https://doi.org/10.1016/j.physb.2003.12.006

Shaaban, E. R., & Tomsah, I. B. (2011). The effect of Sb content on glass-forming ability, the thermal stability, and crystallization of Ge-Se chalcogenide glass. *J. Therm. Anal. Calorim., 105*, 191-198. https://doi.org/10.1007/s10973-011-1317-z

Shaaban, E., Kansal, I., Shapaan, M., & Ferreira, J. (2009). Thermal stability and crystallization kinetics of ternary Se-Te-Sb semiconducting glassy alloys. *J. Therm. Anal. Calorim., 98*, 347-354. https://doi.org/10.1007/s10973-009-0313-z

Starink, M. J. (2003). The determination of activation energy from linear heating rate experiments: a comparison of the accuracy of isoconversion methods. *Thermochim. Acta, 404*, 163-176. https://doi.org/10.1016/S0040-6031(03)00144-8

Starink, M. J., & Zahra, A.-M. (1997). Determination of the transformation exponent s from experiments at constant heating rate. *Thermochim. Acta, 298*, 179-189. https://doi.org/10.1016/S0040-6031(97)00118-4

Tacke, M. (1995). New developments and applications of tunable IR lead salt lasers. *Infrared Physics & Technology, 36*, 447-463. https://doi.org/10.1016/1350-4495(94)00101-P

Tohge, N., Matsuo, H., & Minami, T. (1987). Electrical properties of n-type semiconducting chalcogenide glasses in the system Pb-Ge-Se. *Journal of Non-Crystalline Solids, 95*, 809-816. https://doi.org/10.1016/S0022-3093(87)80685-3

Tripathi, S. K. (2010). Temperature-dependent barrier height in CdSe Schottky diode. *Journal of Materials Science, 45*, 5468-5471. https://doi.org/10.1007/s10853-010-4601-6

Tripathi, S. K., Patial, B. S., & Thakur, N. (2012). Glass transition and crystallization study of chalcogenide Se_{70} Te_{15} In_{15} glass. *J. Therm. Anal. Calorim., 107*, 31-38. https://doi.org/10.1007/s10973-011-1724-1

Turnbull, D., & Fisher, J. C. (1949). Rate of nucleation in condensed systems. *The Journal of Chemical Physics, 17*, 71-73. https://doi.org/10.1063/1.1747055

Vashist, P., Patial, B. S., Bhardwaj, S., Tripathi, S. K., & Thakur, N. (2023). On the non-isothermal crystallization kinetics, glass forming ability and thermal stability of Bi additive Se-Te-Ge alloys. *J. Therm. Anal. Calorim.*, 148, 7717-7726. https://doi.org/10.1007/s10973-023-12271-5

Vyazovkin, S. (2000). Computational aspects of kinetic analysis.: Part C. The ICTAC Kinetics Project – the light at the end of the tunnel? *Thermochim. Acta, 355*, 155-163. https://doi.org/10.1016/S0040-6031(00)00445-7

Vyazovkin, S. (2000). Kinetic concepts of thermally stimulated reactions in solids: a view from a historical perspective. *International Reviews in Physical Chemistry, 19*, 45-60. https://doi.org/10.1080/014423500229855

Vyazovkin, S. (2000). On the phenomenon of variable activation energy for condensed phase reactions. *New Journal of Chemistry, 24*, 913-917. https://doi.org/10.1039/B004279J

Vyazovkin, S. (2003). Reply to "What is meant by the term 'variable activation energy'when applied in the kinetics analyses of solid state decompositions (crystolysis reactions)?". *Thermochim. Acta, 397*, 269-271. https://doi.org/10.1016/S0040-6031(02)00391-X

Vyazovkin, S., & Dranca, I. (2006). Isoconversional analysis of combined melt and glass crystallization data. *Macromolecular Chemistry and Physics, 207*, 20-25. https://doi.org/10.1002/macp.200500419

Wanjun, T., & Donghua, C. (2005). An integral method to determine variation in activation energy with extent of conversion. *Thermochim. Acta, 433*, 72-76. https://doi.org/10.1016/j.tca.2005.02.004

Wilhelm, A. A., Boussard-Pledel, C., Coulombier, Q., Lucas, J., Bureau, B., & Lucas, P. (2007). Development of far-infrared-transmitting Te based glasses suitable for carbon dioxide detection and space optics. *Advanced Materials, 19*, 3796-3800. https://doi.org/10.1002/adma.200700823

Wojciech, W., Kalb, J. A., Wamwangi, D., Steimer, C., & Wuttig, M. (2007). Phase change materials: from structures to kinetics. *Journal of Materials Research, 22*, 2368-2375. https://doi.org/10.1557/jmr.2007.0301

Wuttig, M., & Steimer, C. (2007). Phase change materials: From material science to novel storage devices. *Applied Physics A, 87*, 411-417. https://doi.org/10.1007/s00339-007-3931-y

Wuttig, M., & Yamada, N. (2007). Phase-change materials for rewriteable data storage. *Nature Materials, 6*, 824-832. https://doi.org/10.1038/nmat2009

Wuttig, M., Bhaskaran, H., & Taubner, T. (2017). Phase-change materials for non-volatile photonic applications. *Nature Photonics, 11*, 465-476. https://doi.org/10.1038/nphoton.2017.126

Yoon, S.-M., Lee, N.-Y., Ryu, S.-O., Choi, K.-J., Park, Y.-S., Lee, S.-Y., … Wuttig, M. (2006). Sb-Se based phase-change memory device with lower power and higher speed operations. *IEEE Electron Device Letters, 27*, 445-447. https://doi.org/10.1109/LED.2006.874130

Zakery, A., & Elliott, S. R. (2003). Optical properties and applications of chalcogenide glasses: a review. *Journal of Non-Crystal-Line Solids, 330*, 1-12. https://doi.org/10.1016/j.jnoncrysol.2003.08.064